



Purified Guar Gum as a Sustainable Green Agent for Crude Oil-in-water Emulsions

AYMAN ABUREID¹, SAHL YASIN², FATIMAH ALSAEED³
NASIR A. IBRAHIM⁴ and MOHAMED ALZUBAIR ALMALLEEH⁵

¹Department of Chemical Engineering, Faculty of Engineering and Technology,
University of Gezira, Wad Medani, Sudan.

²Sudanese Chemical Society, Sudan

³Department of General Studies, Almoosa College of Health Sciences, Al Ahsa, Saudi Arabia.

⁴Department of Biology, College of Science, Imam Mohammad Ibn
Saud Islamic University (IMSIU), Riyadh 13318, Saudi Arabia

⁵University of Technology & Applied Science- Rustaq, Oman.

*Correspondence author E-mail: sahyasin@hotmail.com

<http://dx.doi.org/10.13005/ojc/420301>

(Received: February 09, 2026; Accepted: April 01, 2026)

ABSTRACT

Guar gum (GG) is a natural polysaccharide widely used in pharmaceuticals, oilfield applications, and superabsorbent materials due to its hydrocolloid and emulsifying properties. However, its potential as a demulsifier remains underexplored. This study evaluates the reverse demulsification performance of purified guar gum (PGG) as a biodegradable and environmentally friendly alternative for treating crude oil-in-water emulsions without chemical modification. PGG was characterized using FT-IR spectroscopy, elemental analysis, thermogravimetric analysis (TGA), differential thermal analysis (DTA), scanning electron microscopy (SEM), and rheological measurements. The results confirmed its galactomannan structure, thermal stability, and uniform morphology. Reverse demulsification efficiency was applied through bottle tests and UV-Vis spectrophotometry, with performance compared to a commercial reverse demulsifier (RSA-3952N). Emulsion samples obtained from the Central Processing Facility (CPF) in Block 6 of a Sudanese oilfield were used. At a concentration of 0.04% in water, PGG achieved a maximum oil-water separation efficiency of 21%. Although less effective than synthetic demulsifiers, PGG demonstrates significant promise due to its biodegradability, low toxicity, and availability. These findings support its potential as a sustainable solution for petroleum wastewater treatment.

Keywords: Guar gum; Purified guar gum; Galactomannan; Oil-in-water emulsion; Reverse-demulsification.



INTRODUCTION

Hydrocolloids play a significant role in the food industry, as they possess multifunctional properties, serving as thickeners, gelling agents, stabilizers, texturizers, and emulsifiers. They are also used to create edible coatings and enhance the flavor. Hydrocolloids play a crucial role in maintaining the appealing sensory qualities of reformulated fat-reducing food items. Their applications have also expanded into the medical field, where they are prized for providing a variety of health benefits and low-calorie dietary fiber¹. Guar gum (GG) is produced from the endosperm of the guar seed *Cyamopsis tetragonolobus* and *Cyamopsis psoraloides*, belongs to the *Leguminosae* family. It fragments from the shell and reproduces into different particles. However, GG, a remarkable natural polymer derived from guar beans, stands out among hydrocolloids for its exceptional properties and versatile applications². Galactomannan polysaccharide is characterized by its impressive molecular structure, consisting of a linear, 1-4-linked mannose backbone adorned with galactose side chains. This unique configuration contributes to guar gum's exceptional functions in various industries, particularly in the food and pharmaceutical sectors.

One of the most promising features of GG is its extensive range of molecular Weights. Scientific studies have reported that the molecular Weight varies from as low as 50,000 to as high as 8,000,000 g/mol, with some sources indicating an average of approximately 1.8 million Daltons². This extensive range is attributed to GG's origin, processing methods, and potential biodegradation. Moreover, the high molecular Weight of GG places it among the most massive naturally occurring water-soluble polymers, a characteristic that significantly contributes to its potent viscosifying properties³⁻⁴.

As illustrated in Figure 1 above, the chemical structure of guar gum elucidates its remarkable water solubility. The galactose units attached to the mannose backbone facilitate strong interactions with water molecules, enabling guar gum to dissolve readily in cold water without heating. This fundamental property is widely used as an effective thickening agent in numerous applications⁶. GG is used in various petroleum applications, including

as a green corrosion inhibitor in fracturing fluids, a viscosity modifier, and a demulsifier for water emulsions. Additionally, GG is primarily used in drilling fluids and mud solutions and in hydraulic fluids manufacturing. Conversely, its applications for enhanced oil recovery (EOR) are relatively limited⁷⁻⁹. Alkali surfactant polymers were used to improve oil recovery; EOR was a convenient approach for extracting residual oil in the O/W system. Generally, polymers are often utilized to adjust the rheological behavior of injected solutions, enhancing the mobility ratio and consequently boosting the crude oil production rate^{7,8}. GG was applied to enhance oil recovery and high stability at high temperatures (up to 210 °C) and in the presence of high salinity (up to 20% NaCl) in sandstone reservoirs. The results showed that the recovery factor of the experiment exceeded 16% without modifications, as previously reported by Tagwa A. Musa and her co-workers⁷. GG has a good shear thickening, assertive behavior, and is highly stable toward microbial degradation. A new two-fluid system has been developed by adopting bentonite, guar gum, polyanionic cellulose (PAC)", and gum Arabic was prepared by A. O. Olatunde et al. They examine the rheological behavior and filtration loss property under controlled conditions. The results showed that GG exhibits more stable rheological behavior than Arabic gum⁹. On the other hand, Junchi Ma et al. applied guar gum to remove oily sewage in crude oil. They prepared "guar gum stearic hydrazide" (GG-SH) through a condensation reaction. GG-SH has a high affinity for oil, with a removal capacity of 2157.3 mg/g, and the process follows a pseudo-second-order rate law¹⁰.

Previous studies confirm that biodegradable demulsifiers were applied as green agents that effectively break water-in-oil emulsions during crude oil extraction and processing in the industry. Which are categorized by their source and chemical nature table 1 present natural biodegradable demulsifiers

To the best of our knowledge, there are no recent studies examining Purified Guar Gum (PGG) and its potential applications in crude oil emulsion treatment.

GG biopolymer is an eco-friendly, non-toxic, cost-effective, and renewable material widely used as a fracturing fluid agent for oil extraction from reservoirs. In the present study, water-soluble GG

was purified, characterized, and examined for its effectiveness in clarifying and reverse demulsifying crude oil-in-water emulsions.

MATERIALS AND METHODS

Materials

Guar gum, galactomannan content (80-82 %) was obtained from Gitaf Company, Khartoum, Sudan. Ethanol (99.8%) was purchased from Duksan Pure Chemicals, Korea. Industrial-grade ethanol (96%) from the local market. Acetone for synthesis (99.0%) from CDH (Central Drug House Ltd), New Delhi, India. Varsol (naphtha safety solvent) (C9~C11 paraffin 85% + aromatics 15%) was purchased from Recochem Inc., Montreal, Quebec.

Extraction and Purification of Galactomannan Polysaccharide

Purifying guar gum is a crucial step in refining raw guar splits into a purified-grade substance suitable for use across various fields, including food, medical, and industrial applications. The goal of this process is to reduce contaminant amounts, such as residual proteins, fibrous material, husk fragments, and insoluble particles, resulting in a more concentrated and functionally effective galactomannan compound.

The method for purifying guar gum (GG) was adapted by (14) and (5). Initially, 1 gram of guar flour was defatted by twice-washing with acetone at a 1:1 (w/v) ratio. After air-drying, the defatted guar flour was suspended in 100 mL of distilled water and stirred continuously with a glass rod. The resulting suspension was filtered through muslin cloth and centrifuged at 3500 rpm for 15 minutes. 100 mL of absolute ethanol was added to the supernatant liquid. The precipitate, containing fibrous galactomannan polysaccharide, was further washed with acetone. The sample was then air-dried at room temperature and oven-dried at 50°C for 1 hour. For further purification, the extracted polysaccharide was redissolved in distilled water to a concentration of 1 g/100 mL and then clarified by centrifugation at 4000 rpm and 35°C for 20 minutes twice. The supernatant obtained from this process was treated with 100 mL of absolute ethanol, and the purified extract was then further washed with acetone and thoroughly dried at room temperature and in an oven at 50°C for one hour to obtain PGG. Eq. 1 calculated the Percentage

of purified polysaccharide, which is further plotted in Figure 2.

$$\% \text{PP} = \left(\frac{PPW}{EPW} \right) \times 100 \quad \dots(1)$$

Reverse demulsification

Emulsified water samples were collected from West Sudan, Block 6 "Afulla, central processing facility "CPF" - Bleela oilfield, sedimentation tank "1501B", following thorough flushing, a 5-liter sample of emulsified water was obtained, with a recorded temperature of approximately 60°C. The clarifying efficiency of each sample was assessed using the bottle test method. In detail, 100 mL glass-capped measuring cylinders were filled to the mark with emulsified water and labeled 1, 2, and 3, forming three groups. The first group was a blank control sample (a1, b1, and c1), the second group was dosed with industrial reverse demulsifier (RSA-3952N)(a2,b2, and c2), and the third group was dosed with purified guar gum (PGG) solution prepared at a concentration of 0.04%(a3, b3, and c3). To emulsified water samples in the first group dosed with 2.5, 5, and 10 µL, corresponding to 25, 50, and 100 ppm concentrations of oil water, respectively, the same as those in the second group dosed with 2.5, 5, and 10 µL, corresponding to 25, 50, and 100 ppm concentrations of industrial reverse demulsifier (RSA-3952N). Each sample was gently shaken for 50 slow rolls and then transferred to a water bath maintained at 60°C. Visual assessments were conducted immediately and every 10 minutes for a total duration of 30 minutes. The results were categorized based on water quality as shown in Figure 6: "oily," "less oily," or "clear." A successful treatment was indicated by the absence of oil droplets on the glass tube sides and a well-coalesced oil layer. Following the visual assessment, a syringe with a long needle was used to extract a 10 mL portion from the bottom layer of each tube. Those portions were then extracted using the varsol method. The resulting organic layer was analyzed for oil content using a spectrophotometric method. Hach DR6000 calibration curve prepared as a series of standard solutions of known oil concentrations in the same solvent used for extraction (varsol). The absorbance of each standard solution was measured at a wavelength (225 nm where the oil shows good absorbance. Oil-in-water content values

were used to calculate reverse demulsification (deoiling) efficiency using Equation 2 based on UV-Vis spectrophotometer readings, and the results are further plotted in Figures 8 and 9.

$$\%DE = \left(\frac{o/w \text{ blank} - o/w \text{ sample}}{o/w \text{ Blank}} \right) \times 100 \quad \dots(2)$$

Where: %DE = Deoiling Efficiency
O/W = O/W in ppm for the Blank and the sample.

Instrumental Analysis

FT-IR spectra were obtained using a Shimadzu FT-IR 8400 S. CE instrument. Potassium bromide (KBr) discs were prepared by mixing powdered samples with dry KBr in a 1:100 ratio.

The elemental composition (C, H, and N) of purified guar gum (PGG) was determined by using a Vario EL III elemental analyzer. Dried PGG samples (2–3 mg) were combusted at 950 °C in a helium/oxygen atmosphere. The resulting gases were separated by gas chromatography (GC) and detected with a thermal conductivity detector (TCD). The Calibration of the GC was performed using acetanilide standards with triplicate measurements for each sample. Across all measured elements, Thermogravimetric analysis (TGA) and Differential Thermogravimetric Analysis (DTGA) were performed using a Thermo Gravimetric Analyzer (TGA-50, Shimadzu) and a Differential Thermal Analyzer (DTG-60H, Shimadzu).

A Scanning Electron Microscope (SEM, JSM-6610, JEOL, Japan) was used to characterize the external surface and microstructure of the PGG sample at 1500x and 2000x magnifications.

The rheological behavior of a diluted aqueous solution was studied at 25 °C using a Brookfield DV-III Ultra Programmable Rheometer with a Spindle-21. The Density of the same solution was measured using a density bottle. The residual oil in water was measured using a UV-VIS spectrophotometer (HACH DR 6000, Loveland, Colorado, USA).

Three doses (2.5, 5, and 10 µL) were applied to the Blank, PGG, and commercial demulsifier,

respectively. PGG's demulsification performance was validated by using statistical analysis, with means and standard deviations calculated across four replicates. Pairwise comparisons were used to ensure the differences were statistically significant. (e.g., t-tests-ANOVA or Mann-Whitney U tests, depending on data normality) were performed between groups (PGG vs. Blank, PGG vs. commercial), with significance assessed at *p* < 0.05. All analyses were applied in R (v4.4.2) using the stats and rstatix packages.

RESULTS AND DISCUSSION

Purified guar gum (PGG)

Purified guar gum (PGG) extracts presented in Table 2 were calculated using Equation 1. Figure 2 displays the corresponding values, illustrating the yield of extracted galactomannan. The results indicate a consistent decline in the yield of the raw guar gum sample in stand storage over four years, attributed to the degradation of the galactomannan polysaccharide. Additionally, the viscosity of the raw gum decreased significantly, from 129.6 to 1.9 centipoise, corresponding to a galactose-to-mannose ratio of 1:2 after 254 hours (8).

%PP = Percent of purified polysaccharide. PPW = Weight of purified polysaccharide, and EPW = Weight of extracted polysaccharide.

Characterization

FTIR spectra were utilized to confirm the purification of GG. In polysaccharides, the absorption band around 1600 cm⁻¹ corresponds to the asymmetric stretching vibration of the (C=O) group. Peaks in the stretching region of PGG indicate the presence of amides, supporting the approximation analysis findings that suggest the presence of protein moieties in pure guar gum samples. Additionally, the broad and strong peak at 3400 cm⁻¹ is frequently attributed to (-OH) bond stretching. The band near 1400 cm⁻¹ is associated with the symmetric stretching of the (-COO) group, a characteristic feature of galactomannan polysaccharides, as shown in Figure 3. Lastly, the medium sharp peak around 2900 cm⁻¹ arises from (C-H) stretching vibrations related to the ring methine hydrogen atoms. Additional results are provided to support the first method¹¹⁻¹². This result is consistent with the previous study of Elsaheed and her co-workers¹³.

Table 1: Natural biodegradable demulsifiers

S. No	Green biodegradable sources	Demulsifier
1	polysaccharide-based demulsifiers	guar gum derivatives, Chitosan, and Alginate
2	Protein-Based Demulsifiers	Soybean Protein Isolate (SPI), and Whey Protein
3	Plant-Based Surfactants	Saponins and Lecithin.
4	Microbial/Bio-Based demulsifiers	Rhamnolipids and Sophorolipids.
5	Lignin Derivatives;	Sulfonated Lignin
6	Fatty acid-based	LA1 and LA2

Table 2: (PGG) Extracts present data on raw guar gum, purified gum, purification percentage, and product codes, categorized by year

Raw guar gum Weight in grams	Purified guar gum Weight in grams	% of purified guar	Product code	Year
1	0.805	80.5	PGG1	2018
1	0.550	55.0	PGG2	2019
1	0.439	43.9	PGG3	2020
1	0.310	31.05	PGG4	2021

Table 3: The elemental analysis presents the atomic mass percentage within the structural unit of the PGG specimen, along with its viscosity and Density at ambient temperature

PGG sample	C	H	N	O	Viscosity in Centipoise at 25 °C	Density g/cm ³
% Atomic mass	38.98	7.49	1.14	52.39	34	0.3757
Mole ratios	3.245	7.483	0.0814	3.274	-	-

Table 4: Viscosity and Density for (PGG 0.04%) and industrial reverse demulsifier (RSA-3952N) at ambient temperature

Sample	Viscosity in Centipoise °C at 25	Density g/cm ³
PGG	34	0.38
RSA	87	1.23

For elemental analysis, the oxygen content (O) was calculated by subtracting the percentages of carbon (C), hydrogen (H), and nitrogen (N) from the total (100%). The mole ratios were determined by dividing the Weight percentage of each element by its respective atomic mass, leading to the empirical formula CH O. This result aligns with the assumption that purified galactomannan polysaccharides can be

extracted. The trace amount of nitrogen reported in Table 3 can likely be attributed to the proteinaceous content in the raw guar gum (14), (15).

For TGA analysis (Figure 4a), a 16.35 mg sample of purified guar gum (PGG) exhibited three main Weight loss zones on the thermogram curve. The initial Weight loss between 28.77°C and 201.09°C is attributed to moisture evaporation. The second zone, spanning 201.62°C to 398.38°C, is likely due to the degradation of the polymeric backbone, which contains functional (-OH) groups. The third zone, observed between 398.24°C and 544.59°C, corresponds to the breakdown of the polymer backbone featuring (-CH₂OH) groups. The decomposition process involves a series of events where galactose and mannose units detach from the guar gum backbone. (16). Figure 4 illustrates that

Table 5: Visual and spectrophotometric evaluation of purified guar gum clarification (deoiling) efficiency

Sample code - Dilution %	Doses in μ l	Visual evaluation	Spectrophotometric evaluation	
			O/W in ppm	%DE
(1) PGG - 0.04%	2.5	O	320	13.3
	5	L/O	277.5	18.4
	10	L/O	244.8	21
(2) (RSA-3952N)	2.5	C	40	89.2
	5	C	58.8	82.8
	10	C	44	85.8
(3) Blank	2.5	O	369	0
	5	O	340	0
	10	O	310	0

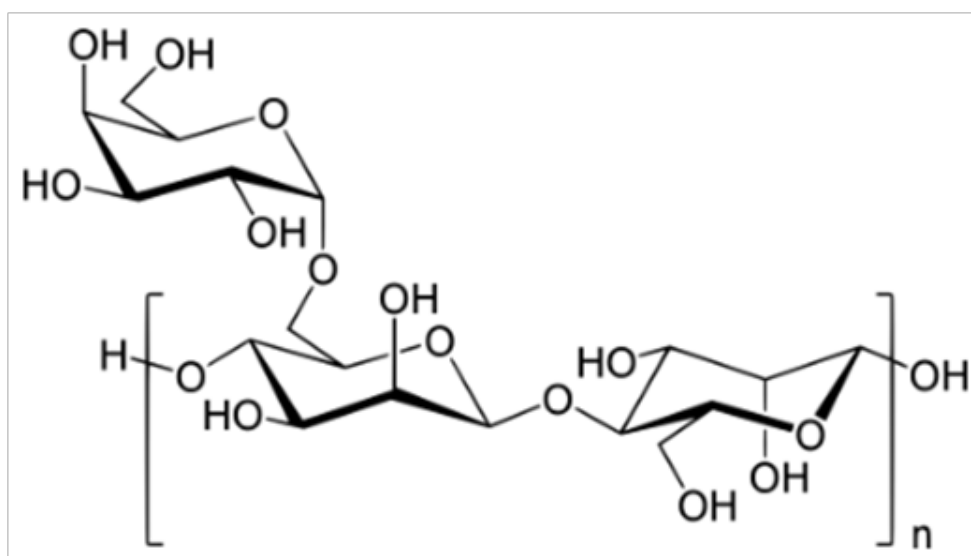
the total Weight reduction of the sample was 16.291 mg, corresponding to 99.612% of the initial Weight. The Weight losses in the three zones were 1.624 mg (9.932%), 11.883 mg (72.659%), and 2.785 mg (17.031%), respectively. The peak temperatures for each zone, determined from differential thermal analysis (DTA) curves, were 90.80 °C, 302.62 °C, and 455.79 °C, as shown in Figure 4 b. Additional results are provided in supporting information.

SEM analysis of PGG revealed notable structural characteristics. At 15000x and 2000x magnification, with particle sizes of 207 μ m and 27.6 μ m, respectively, the sample displayed an

amorphous structure comprising multiple layers and irregular, fragmented sheets. At 15000x magnification, a rough topography with visible cracks and a granular composition was observed, as shown in Fig 5a. The glittering surface became more pronounced, indicating the preserved structural integrity of PGG (17), (18).

Rheological Behavior

Rheological behavior is the study of the flow and deformation of materials under external forces. The regular structure of the long-branched chains in PGG contributes to its ability to form a highly viscous solution even at low concentrations.

**Fig. 1: The Chemical Structure of Guar Gum (5)**

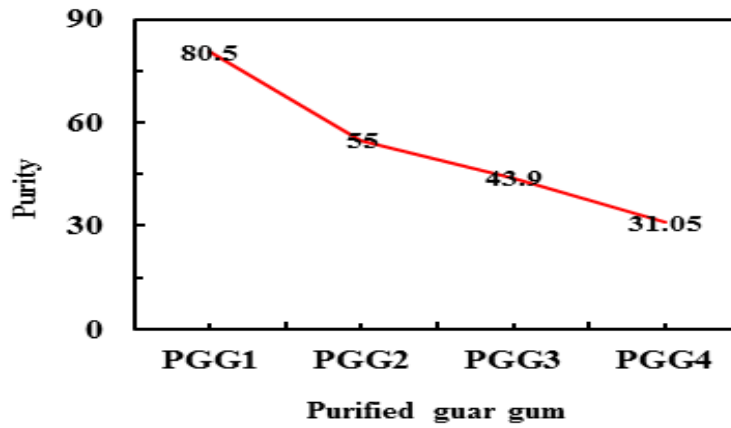


Fig. 2: Typical (PGG) samples yield from 2018 to 2023

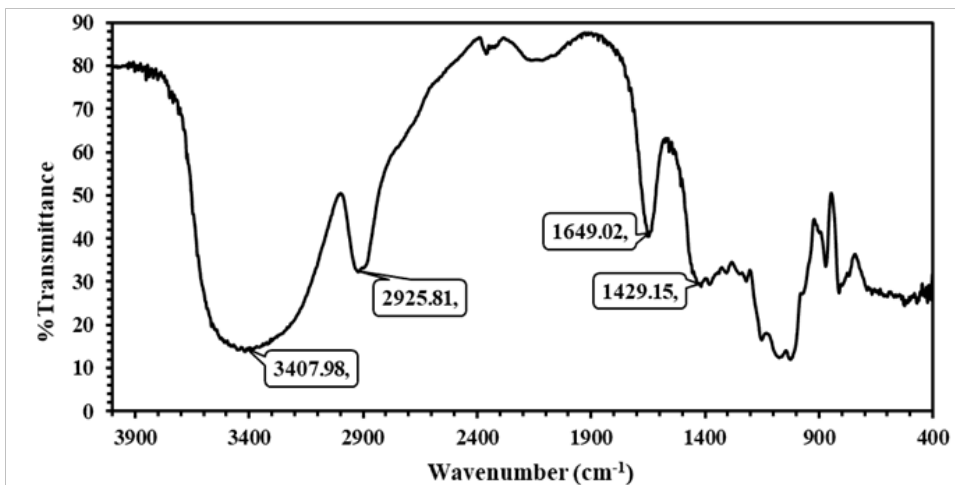


Fig. 3: The FTIR spectrum displays prominent peaks corresponding to the functional groups in the PGG sample

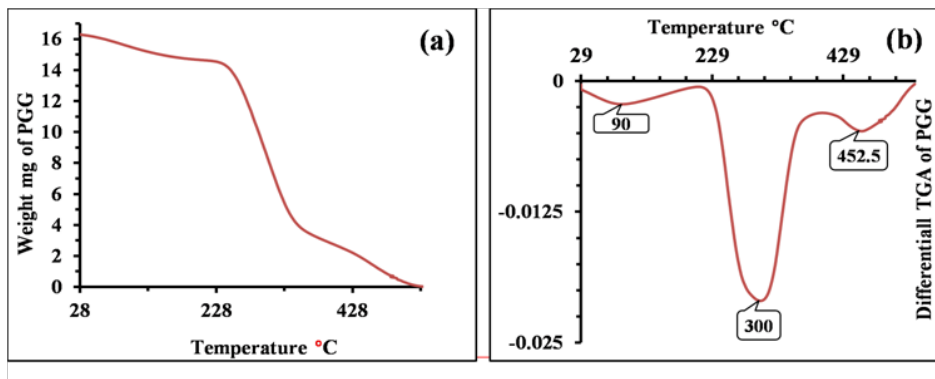


Fig. 4: Thermogram (a) and its corresponding differential thermogram (b) of PGG conducted at the range of 0.00°C to 600°C

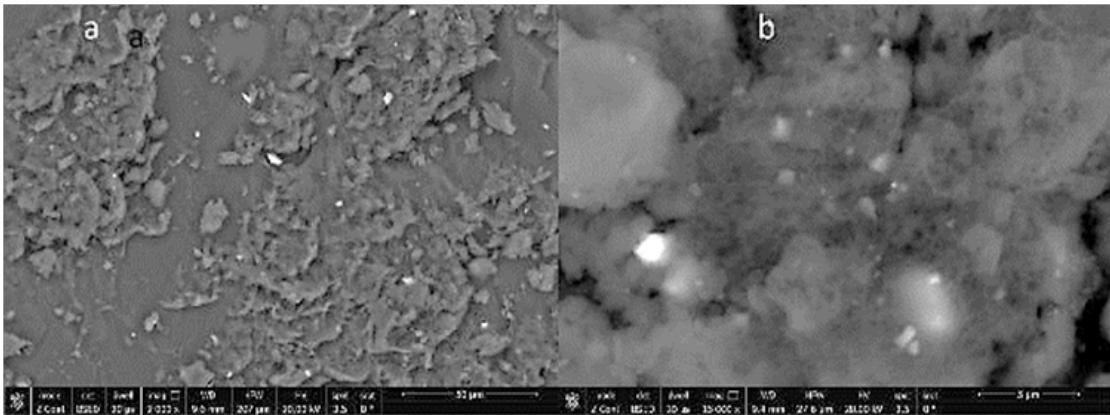


Fig. 5: SEM images of PGG at different magnifications (a) 2000x and (b) 15000x, scale bar 2, and 1.5 μm (revealing surface cracks)

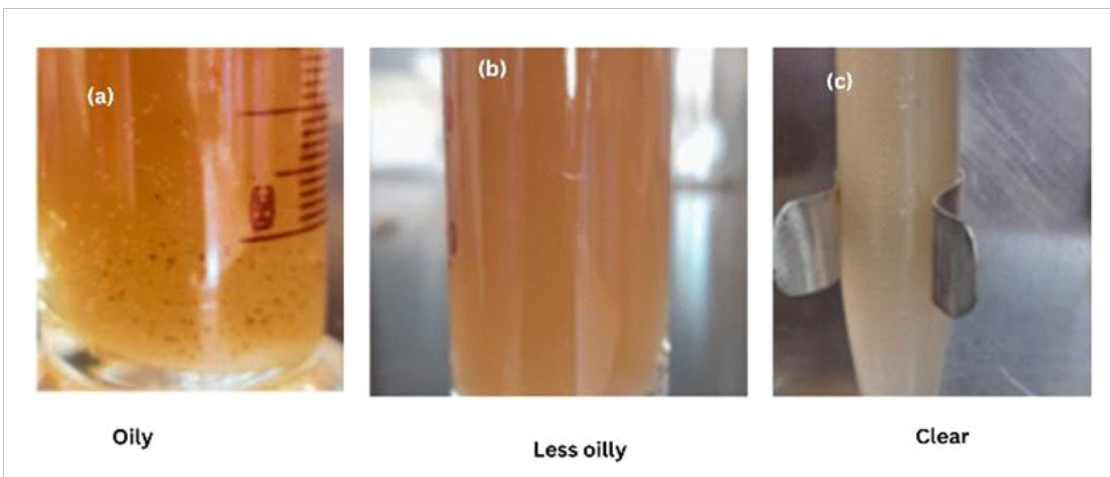


Fig. 6: Visual evaluation criteria for reverse demulsification efficiency where a – oily oil drops, b - less oily, and c is present, Clear

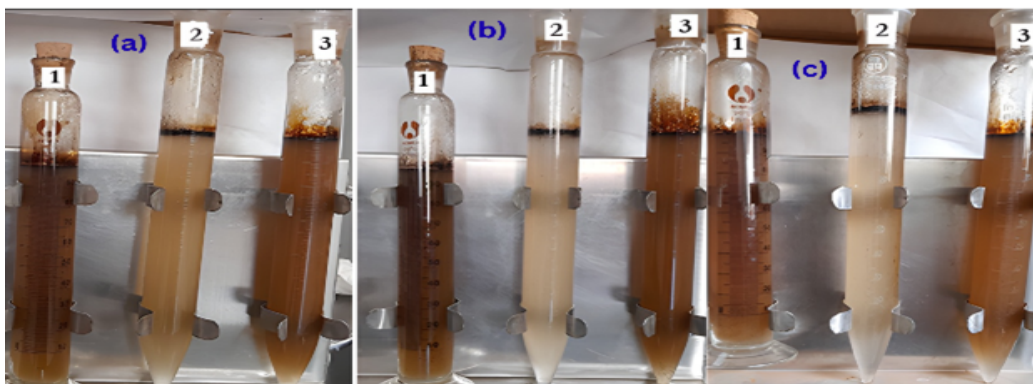


Fig. 7: Does 25, 50, and 100 ppm indicate by notations a, b, and c. Numbers 1, 2, and 3 corresponded to a blank, industrial demulsifier (RSA-3952N) and purified guar gum (PGG), respectively. The composition of emulsions is shown in Table 5

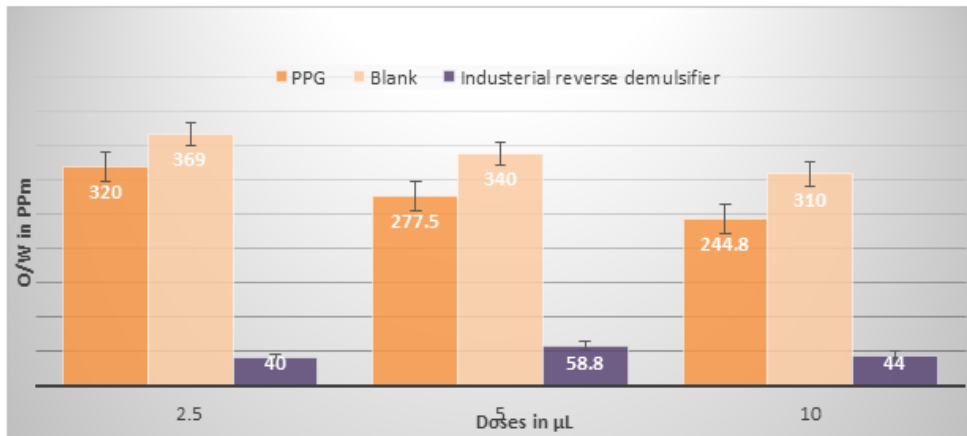


Fig. 8: Spectrophotometric evaluation results of Blank, PPG, and industrial reverse demulsifier, presented in three portions at concentrations of 2.5, 5, and 10

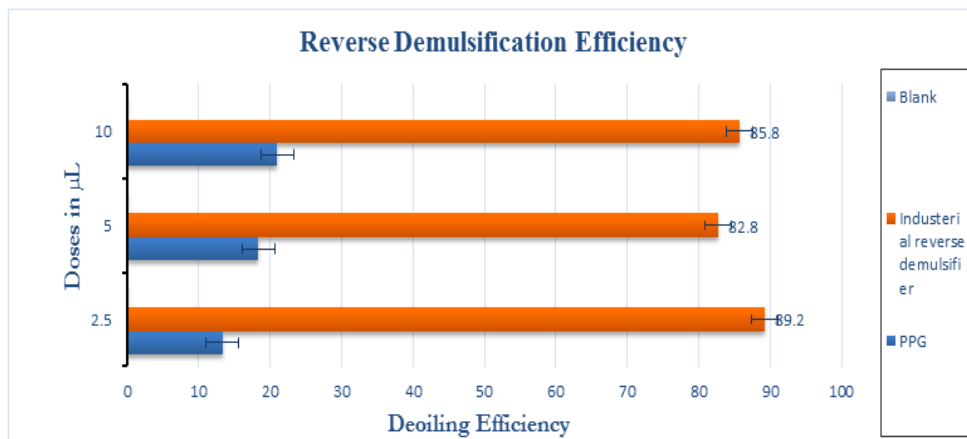


Fig. 9: Deoiling Efficiency Compared to Industrially Used Reverse Demulsifier

In an aqueous medium, PGG exhibits pseudoplastic or shear-thinning behavior, characterized by a decrease in viscosity with increasing shear rate. As shown in Table 4, when compared to an industrial reverse demulsifier (RSA-3952N). Practically, the PGG sample diluted to 0.04% was tested at 25°C using Spindle-21, yielding a torque of 17% at 250 rpm¹⁹⁻²¹.

Reverse Demulsification Visual and Spectrophotometric Evaluation

The effectiveness of any analytical method for assessing oil-in-water (O/W) emulsions largely depends on the quality of the simulated effluent sample. In this study, the efficiency of reverse demulsification was evaluated using a modified version of the coagulation–flocculation jar test,

commonly referred to as the bottle test²².

A 100 mL volume of emulsified water was used in each experiment and treated with different concentrations (25, 50, and 100 ppm) of purified guar gum (PGG), the industrial demulsifier RSA-3952N (RSA), and a blank control. Initially, all treated samples were visually assessed for water quality and categorized into three levels: Oily (O), Less-oily (L/O), and Clear (C), as illustrated in Figure 6. This classification was based on the visual observation of oil droplet behavior within the glass container. Samples labeled as Oily exhibited a high oil content, with oil droplets clearly visible and adhering to the inner walls of the test tube. In Less-oily samples, the amount of dispersed oil was significantly lower, resulting in fewer or smaller oil droplets, with minimal

adhesion to the tube walls. Clear samples showed no visible oil droplets, indicating effective separation and minimal residual oil content in the water phase. This qualitative assessment was followed by spectrophotometric analysis to determine oil concentration (ppm) via UV-Vis absorbance measurements.

Several mechanisms are involved in achieving effective reverse demulsification or clarification, including polymer bridging, surface adsorption, and charge neutralization via electrostatic patch effects.²³

As shown in Figure 7, the doses—25, 50, and 100 ppm—corresponded to a, b, and c, respectively, and were applied to three sample types: the Blank, RSA, and PGG labeled as 1, 2, and 3, respectively, each treated with a constant volume of 2.5 μL of water containing oil.

At the low dose (25 ppm), the PGG-treated sample exhibited visible oil droplets adhered to the inner glass surface and was categorized as Oily. The RSA-treated sample showed fewer oil droplets and appeared turbid, while the blank sample also retained its Oily water quality.

At the medium dose (50 ppm), oil droplets were no longer emulsified in the PGG-treated sample; therefore, it is considered less oily. The RSA-treated sample appeared Clear, while the blank sample remained Oily.

At the highest dose (100 ppm), both PGG- and RSA-treated samples exhibited no visible oil droplets and were considered less oily, whereas the blank sample was visible as oily water. These observations are consistent with previous studies, indicating that optimal clarification is achieved when the polyelectrolyte dose is sufficient to neutralize surface charges or reduce the zeta potential toward zero, thereby reaching the isoelectric point²⁴⁻²⁵.

Theoretically, the zeta potential represents the electric potential of a dispersed particle or droplet within the interfacial double layer relative to a point in the continuous phase distant from the interface. Van der Waals forces tend to induce particle aggregation, destabilizing the colloidal suspension²⁰. However,

excessive polymer doses can result in charge reversal, leading to particle redistribution with a positive charge instead of a negative charge²⁶.

Spectrophotometric evaluation of samples treated with doses of 2.5 μL (25 ppm), 5 μL (50 ppm), and 10 μL (100 ppm) showed decreasing oil-in-water concentrations in UV-VIS spectrophotometer readings for purified guar gum (PGG) samples as the dose volume increased (2.5–10 μL), calculated using Eq. 2. While the oil-in-water concentration for PGG samples was not higher than the Blank, suggesting the absence of emulsion formation, nearly all PGG doses exhibited some clarification characteristics, as shown in Table 5, Figure 8, and Figure 9.

The results demonstrate that industrial reverse demulsifier (RSA-3952N) achieved the highest clarification efficiency (89.2% at 2.5 μL), with consistently low oil-in-water (O/W) concentrations (40–58.8 ppm) and clear phase separation, indicating effective clarification likely due to optimal charge neutralization or interfacial activity. In contrast, purified guar gum (PGG) exhibited moderate clarification efficiency (13.3–21% DE), reducing O/W levels (320–244.8 ppm) with increasing doses but only achieved partial clarification, suggesting limited capability. The blank sample showed no clarification (0% DE, 310–369 ppm O/W), confirming the need for a clarifying aid. Theoretically, the industrial demulsifier's superior performance may arise from the effective reduction of zeta potential, thereby counteracting Van der Waals forces. In contrast, PGG's plateau in efficiency (~21%) implies insufficient interfacial coverage or charge modification. These findings highlight a trade-off between natural polymers, such as PGG, which offer clarification, and synthetic alternatives, such as RSA-3952N, which deliver robust performance at low doses. The results align with literature data, recently Alsaeed and her co-workers were applied two types of polychelates based on graft copolymerization of guar gum for enhancing oil recovery EOR in high salinity condition. In secondary and tertiary, the maximum oil recovery was 70.53 and 72.11% respectively¹³.

A comprehensive statistical assessment was conducted to evaluate the demulsification performance of purified guar gum (PGG) compared

with a commercial demulsifier (RSA-3952N) and a blank. Four replicated trials were used to calculate the mean oil-in-water (O/W) concentrations and related standard deviations. PGG demonstrated a statistically significant reduction in O/W concentration (280.8 ± 21.7 ppm) relative to the blank group (339.7 ± 17.3 ppm; $p = 0.032$, independent samples t-test), though it exhibited remarkably lower efficacy compared to RSA-3952N (47.6 ± 5.5 ppm; $p = 0.008$). One-way ANOVA revealed a significant dose-dependent variation in performance ($F(2,6) = 45.2$, $p < 0.001$), which was further confirmed by Tukey's post hoc test. This indicated moderate demulsification efficiency (13.3–21%) by PGG at elevated concentrations. Assumptions of normality and homoscedasticity were met, as verified by the Shapiro-Wilk and Levene's tests, respectively, thus confirming the statistical validity of the analysis. Collectively, these findings support PGG's potential as an eco-friendly demulsifier; however, its variable performance underscores the need for further formulation and optimization to achieve industrial-grade consistency.

Compared to other green demulsifiers such as Chitosan and tannin-based polymers, guar gum (PGG) exhibits moderate efficiency, achieving 13–21% separation under optimal conditions. Green, eco-friendly demulsifiers based on fatty acids, prepared by Yogesh Dhandh and his co-workers, exhibit results showing that, at 70 for 90 min, the demulsifier achieves 100% separation compared to the commercial one. Chitosan derivatives, such as Fe₃O₄-Chitosan Nanocomposites, have demonstrated higher separation rates, often exceeding 85%, due to Chitosan's strong hydrophobicity and cationic properties. Similarly, tannin-based agents show improved interfacial activity and faster demulsification kinetics. Thus, while PGG is biodegradable and accessible, its lower performance highlights the need for structural modification or synergistic formulations²⁷⁻²⁹.

The manuscript's findings highlight several strengths, including the demonstration that purified guar gum (PGG) at a low concentration of 0.04% is a sustainable, biodegradable alternative for treating crude oil-in-water emulsions, achieving moderate de-emulsification efficiency (up to 21%) with dose-dependent improvements. Comprehensive characterization techniques (FT-IR, TGA, and SEM)

validated PGG's galactomannan structure and stability, while comparative benchmarking against a synthetic reverse demulsifier (RSA-3952N) provided clear performance insights, emphasizing its potential as a greener solution despite lower efficiency. The study's focus on industrial applicability, particularly in oilfield operations, underscores its relevance for advancing eco-friendly demulsification technologies.

CONCLUSION

This study demonstrates that extracting galactomannan polysaccharide from guar gum is feasible, and repeated extractions yield a purified product (PGG). It is important to note that the pure galactomannan polysaccharide content decreases over time due to biodegradation. Moreover, the study demonstrates that emulsified water generated in oil fields can be effectively reverse demulsified using low concentrations and minimal doses of PGG, offering significant environmental and economic advantages. Furthermore, the industrial reverse demulsifier (RSA-3952N) yielded superior visual and spectrophotometric results, achieving the highest clarifying efficiencies. Guar gum biodegradability suggests that fine-grades or selectively purified guar gum will have significant efficiency, which could be further developed through functionalization and derivatization to achieve eco-friendly clarification and reverse demulsification (deoiling) operations. Globally, numerous bio-based clarifying agents and flocculants have been developed and employed to treat wastewater. However, guar gum-based bio-flocculants require further laboratory-scale evaluation and optimization, with particular attention to the effects of molecular Weight and charge density distribution on their efficacy in reverse demulsification of crude oil-in-water emulsions. This study highlights the potential of advancing purified guar gum derivatives, such as guar gum grafted with acrylates or guar gum nanoparticle formulations, to further reduce oil concentrations (ppm) in wastewater from oil fields.

Author Contributions

Ayman Abureid, conceptualization, formal analysis, and writing original draft preparation; Ayman Abureid, Sahl Yasin, Fatimah, and Nasser Ibrahim, and Mohamed Alzubear review, and editing. Ethical Considerations: Not applicable. Consent to Participate: Not applicable.

Consent for Publication: Not applicable

Funding: Not applicable

Conflicting Interests declaration

The authors declare that they have no financial interests or personal relationships that could have influenced the findings presented in this study.

Data Availability Statement

The data are available from the corresponding author upon reasonable request.

ACKNOWLEDGMENTS

The authors extend their appreciation to the Central Research Laboratories, University of Khartoum, Sudan. Special thanks are also due to Dr. Ibrahim Yahia from King Fahd University of Petroleum and Minerals for his insightful guidance and assistance. We extend our sincere acknowledgment to Dr. Mohammed Munawar from the Holy Makkah Food Safety Laboratory for his valuable assistance and support.

REFERENCES

- Nussinovitch A, Hirashima M. Cooking innovations using hydrocolloids for thickening, gelling, and emulsification. Vol. 91, CRC Press. **2013**. 275–285 p.
- Elias H-G. Determination of Molecular Weight and Molecular-Weight Distribution. In: *Macromolecules* [Internet]. Springer US; **1977** [cited 2025 May 25]. p. 297–369. Available from: https://link.springer.com/chapter/10.1007/978-1-4615-7364-7_9
- Kawamura Y. GUAR GUM Chemical and Technical Assessment.*Pas Un Vrai Artic.* **2008**; *1(4)*:2–5.
- Mudgil D, Barak S, Khatkar BS. Guar gum: Processing, properties and food applications - A Review. *J Food Sci Technol.* **2014**; *51(3)*: 409–18.
- Mulimani VH, Prashanth SJ. Investigating plant galactomannans. *Biochemistry and Molecular Biology Education.* **2002**; *30*. 101–3.
- Hussein HAS, Habbani DFI, Hassona DRK. Study of chemical and physical properties of irradiated Guar Gum. Vol. 46, Atomic Energy Research Coordination Council, Sudan Academy of Sciences (SAS), Khartoum (Sudan)). **2012**.
- Musa TA, Ibrahim AF, Nasr-EI-Din HA, Hassan AM. New insights into guar gum as environmentally friendly polymer for enhanced oil recovery in high-salinity and high-temperature sandstone reservoirs. *J Pet Explor Prod [Internet]*. **2021**; *11(4)*:1905–13. Available from: <https://doi.org/10.1007/s13202-020-01080-3>
- Da Silva DA, de Paula RCM, Feitosa JPA. Graft copolymerisation of acrylamide onto cashew gum. *Eur Polym J.* **2007**; *43(6)*:2620–9.
- Olatunde AO, Usman MA, Olafadehan OA, Adeosun TA, Ufot OE. IMPROVEMENT OF RHEOLOGICAL PROPERTIES OF DRILLING FLUID USING LOCALLY BASED MATERIALS. *Pet Coal [Internet]*. 2012 [cited 2025 May 25]; *54(1)*:65–75. Available from: https://www.academia.edu/download/94144922/pc_1_2012_tunde_147_0.pdf
- Ma J, Gu Y, Ma D, Lu W, Qiu J. Acylhydrazone-modified guar gum material for the highly effective removal of oily sewage. *Arab J Chem [Internet]*. **2023**; *16(3)*:104532. Available from: <https://doi.org/10.1016/j.arabjc.2022.104532>
- Sadeghi M, Mohammadinasab E, Shafiei F, Mansouri L, Shasavari H. Grafting copolymerization of hydrophilic monomers onto alginate for modification it's structure. *Orient J Chem.* **2014**; *30(1)*:247–53.
- Sen G, Mishra S, Jha U, Pal S. Microwave initiated synthesis of polyacrylamide grafted guar gum (GG-g-PAM)-Characterizations and application as matrix for controlled release of 5-amino salicylic acid. *Int J Biol Macromol.* **2010**; *47(2)*: 164–70.
- Elsaeed Shimaa SM, Zaki EG, Omar WAE, Ashraf Soliman A, Attia AM. Guar Gum-Based Hydrogels as Potent Green Polymers for Enhanced Oil Recovery in High-Salinity Reservoirs. *ACS Omega.* **2021**; *6(36)*:23421–31.

14. Cunha PLR, Paula RCM d., Feitosa JPA. Purification of guar gum for biological applications. *Int J Biol Macromol [Internet]*. **2007** [cited 2024 Dec 9];41(3):324–31. Available from: <https://www.sciencedirect.com/science/article/pii/S0141813007001067>
15. Pal S, Mal D, Singh RP. Synthesis and characterization of cationic guar gum: A high performance flocculating agent. *J Appl Polym Sci*. **2007**;105(6): 3240–5.
16. Sharma RK, Lalita. Synthesis and characterization of graft copolymers of N-Vinyl-2-Pyrrolidone onto guar gum for sorption of Fe²⁺ and Cr⁶⁺ ions. *Carbohydr Polym [Internet]*. **2011**;83(4):1929–36. Available from: <http://dx.doi.org/10.1016/j.carbpol.2010.10.068>
17. Qiu L, Shen Y, Wang C, Yang X. Scanning electron microscopy analysis of guar gum in the dissolution, gelation and gel-breaking process. *Polym Test [Internet]*. **2018**; 68(February):95–9. Available from: <https://doi.org/10.1016/j.polymertesting.2018.04.001>
18. Wang Q, Ellis PR, Ross-Murphy SB. Dissolution kinetics of guar gum powders - II. Effects of concentration and molecular weight. *Carbohydr Polym [Internet]*. **2003** [cited 2025 May 26];53(1):75–83. Available from: <https://www.sciencedirect.com/science/article/pii/S0144861703000092>
19. Shobha MS, Tharanathan RN. Rheological behaviour of pullulanase-treated guar galactomannan on co-gelation with xanthan. *Food Hydrocoll [Internet]*. **2009** [cited 2025 May 26];23(3):749–54. Available from: <https://www.sciencedirect.com/science/article/pii/S0268005X0800088X>
20. Chenlo F, Moreira R, Silva C. Rheological behaviour of aqueous systems of tragacanth and guar gums with storage time. *J Food Eng [Internet]*. **2010** [cited 2025 May 26]; 96(1): 107–13. Available from: <https://www.sciencedirect.com/science/article/pii/S0260877409003525>
21. Zhang M, He J, Deng M, Gong P, Zhang X, Fan M, et al. Rheological behaviours of guar gum derivatives with hydrophobic unsaturated long-chains. *RSC Adv*. **2020**; 10(53):32050–7.
22. Glaser RA, Shulman S, Klinger P. Data Supporting a Provisional American Society for Testing and Materials (ASTM) Method for Metalworking Fluids, Part 2: Preliminary Report of Evaluation of a Ternary Solvent Blend in a Provisional ASTM Method for Metalworking Fluids (P-42-97). *J Test Eval [Internet]*. **1999** [cited 2024 Dec 9];27(2):131–6. Available from: <https://asmedigitalcollection.asme.org/testingevaluation/article/27/2/131/1188845>
23. Gregory J, Barany S. Adsorption and flocculation by polymers and polymer mixtures. *Adv Colloid Interface Sci [Internet]*. **2011** Nov 14 [cited 2025 Aug 23]; 169(1):1–12. Available from: <https://www.sciencedirect.com/science/article/abs/pii/S0001868611001229>
24. Bolto B, Gregory J. Organic polyelectrolytes in water treatment [Internet]. Vol. 41, *Water Research*. **2007** [cited 2024 Dec 9]. p. 2301–24. Available from: <https://www.sciencedirect.com/science/article/pii/S0043135407001881>
25. Kleimann J, Gehin-Delval C, Auweter H, Borkovec M. Super-stoichiometric charge neutralization in particle-polyelectrolyte systems. *Langmuir*. **2005**; 21(8):3688–98.
26. Ahmad AL, Ismail S, Bhatia S. Optimization of coagulation-flocculation process for palm oil mill effluent using response surface methodology. *Environ Sci Technol*. **2005**;39(8):2828–34.
27. Khormali A. Increasing the Efficiency of Demulsification Treatment in Petroleum Industry Using a Multicomponent Demulsifier Package. *Pet Chem [Internet]*. **2023** May 1 [cited 2025 Jul 5];63(5):539–52. Available from: <https://link.springer.com/article/10.1134/S0965544123030210>
28. Dhandhi Y, Kumar Saw R, Singh R, Naiya TK. Application of a novel surface-active green demulsifier for demulsification of field crude oil emulsion. *Sep Sci Technol [Internet]*. **2023** [cited 2025 Jul 6];58(9):1654–78. Available from: <https://www.tandfonline.com/doi/abs/10.1080/01496395.2023.2198108>
29. Kazemi Z, Ghiasi R, Jamehbozorgi S. A theoretical study of the influence of solvent polarity on the structure and spectral properties in the interaction of C 20 and Si 2 H 2. *J Nanoanalysis [Internet]*. **2019**; 6(2):121–8. Available from: <http://creativecommons.org/licenses/by/4.0/>.